

Interspecies organogenesis generates autologous functional islets

Tomoyuki Yamaguchi^{1*}, Hideyuki Sato^{1*}, Megumi Kato-Itoh¹, Teppei Goto², Hiromasa Hara², Makoto Sanbo², Naoaki Mizuno¹, Toshihiro Kobayashi^{1†}, Ayaka Yanagida¹, Ayumi Umino¹, Yasunori Ota³, Sanae Hamanaka¹, Hideki Masaki¹, Sheikh Tamir Rashid^{4,5}, Masumi Hirabayashi² & Hiromitsu Nakauchi^{1,5}

Islet transplantation is an established therapy for diabetes. We have previously shown that rat pancreata can be created from rat pluripotent stem cells (PSCs) in mice through interspecies blastocyst complementation. Although they were functional and composed of rat-derived cells, the resulting pancreata were of mouse size, rendering them insufficient for isolating the numbers of islets required to treat diabetes in a rat model. Here, by performing the reverse experiment, injecting mouse PSCs into Pdx-1-deficient rat blastocysts, we generated rat-sized pancreata composed of mouse-PSC-derived cells. Islets subsequently prepared from these mouse-rat chimaeric pancreata were transplanted into mice with streptozotocin-induced diabetes. The transplanted islets successfully normalized and maintained host blood glucose levels for over 370 days in the absence of immunosuppression (excluding the first 5 days after transplant). These data provide proof-of-principle evidence for the therapeutic potential of PSC-derived islets generated by blastocyst complementation in a xenogeneic host.

Organ transplantation remains the only cure for a growing number of patients suffering from a broad range of debilitating and fatal diseases. An increasing clinical burden with continued donor deficiency means that, for example, over 76,000 patients in the US are currently waiting for a transplant operation (<https://optn.transplant.hrsa.gov/>). PSCs offer the possibility of addressing this challenge through laboratory generation of unlimited quantities of replacement cells and tissues. Despite advances in deriving organ-specific cells^{1–5} or miniature organs (organoids)^{6–10}, *ex vivo* generation of whole organs that are truly representative of their *in vivo* counterparts remains elusive. Addressing this challenge, we previously reported the generation of whole organs from donor PSCs using their chimaera-forming ability to complement organogenesis-disabled host animals *in vivo*¹¹. We termed this organ generation strategy ‘conceptus complementation’ and, when donor cells are delivered to the recipient at the pre-implantation stage, ‘blastocyst complementation’¹². Rat pancreata generated in mice were structurally and functionally identical to their mouse *in vivo* counterparts, including in size, although supporting tissues (blood vessels and stroma) were a mixture of rat and mouse cells. The effects of transplanting xenogenic supporting tissue into a mouse recipient remained uncharacterized because we could not isolate enough rat islets for transplantation from mouse-sized pancreata. We were thus unable to answer the important question of whether organs generated in a xenogeneic environment by blastocyst complementation could functionally rescue diseased hosts, despite the presence of xenogenic cells. Pancreatic islet transplantation for severe diabetes provides a clinically relevant model to address this question^{13–15}. We therefore sought to determine whether mouse pancreatic islets isolated from pancreata derived in rats through interspecies blastocyst complementation (denoted as mouse^R) could induce long-term glycaemic control in mice with streptozotocin (STZ)-induced diabetes.

Generation of apancreatic rats

Figure 1a shows a schematic representation of the experimental design. Pdx-1-deficient blastocysts were complemented with mouse

PSCs (mPSCs) to generate mouse-derived pancreata in rats (mouse^R pancreata). Islets isolated from these pancreata (mouse^R islets) were then transplanted into mice with STZ-induced diabetes to evaluate their effects on blood glucose regulation. We first generated apancreatic rat blastocysts using genome-editing technology. As the coding region of *Pdx1* is highly conserved between mouse and rat (DNA, 93% homology; amino acid, 93% homology) and the homeo domain is identical in rat and mouse, we predicted *Pdx1* to be the master regulator gene responsible for pancreata development in both rats and mice^{16,17}.

Mutations in the *Pdx1* coding region were achieved, as previously described¹⁸, by injecting into the male pronuclei of rat zygotes *in vitro* transcribed mRNA of *Pdx1* TALEN (transcription-activator-like effector nuclease) and rat ExoI (3 or 10 ng μl⁻¹ of each mRNA) targeted to loci 3 base pairs (bp) and 35 bp downstream of the *Pdx1* initiation codon (Fig. 1b, Table 1). We obtained four mutant rats (*Pdx1*^{+/*mu*}) (5%) from the group injected with 3 ng μl⁻¹, three *Pdx1*^{+/*mu*} rats (9%) from the group injected with 10 ng μl⁻¹, and no homozygous mutant rats (Table 1). Genotyping revealed four different types of *Pdx1* mutants (denoted as A to D). We chose the frameshift mutants A and B for further work: each introduced a stop codon into the middle of the *Pdx1* coding region, at the 30th and 28th amino acids, respectively (Fig. 1c).

As we could not rule out the possibility of mosaicism in first-generation rats, we used second-generation rats generated by crossing two different heterozygous mutants for our downstream complementation assays. We hypothesized that this would not only eliminate mosaicism, but also reduce the influence of off-target effects. To confirm this, we sequenced the 22 sites predicted by the TALENoffer software and demonstrated the absence of indels in *Pdx1*^{+/*mu*A} and *Pdx1*^{+/*mu*B} F₁ rats¹⁹ (Extended Data Table 1). Homozygous mutant rats were born at frequencies corresponding to Mendelian rules. All of them displayed an apancreatic phenotype and all died within 3 days of birth (Fig. 1d, Extended Data Fig. 1a). The predicted amino acid sequences of full-length cDNAs generated from *Pdx1*^{*mu*A/*mu*B} duodenum-derived

¹Division of Stem Cell Therapy, Center for Stem Cell Biology and Regenerative Medicine, Institute of Medical Science, University of Tokyo, Minato-ku, Tokyo, Japan. ²Center for Genetic Analysis of Behavior, National Institute for Physiological Sciences, Okazaki, Aichi, Japan. ³Department of Pathology, Research Hospital, Institute of Medical Science, University of Tokyo, Minato-ku, Tokyo, Japan. ⁴Centre of Stem Cells and Regenerative Medicine and Institute of Liver Studies, King's College London, UK. ⁵Institute for Stem Cell Biology and Regenerative Medicine, Department of Genetics, Stanford University School of Medicine, Stanford, California, USA. †Present address: Wellcome Trust/ Cancer Research UK Gurdon Institute, University of Cambridge, Cambridge, UK.

*These authors contributed equally to this work.

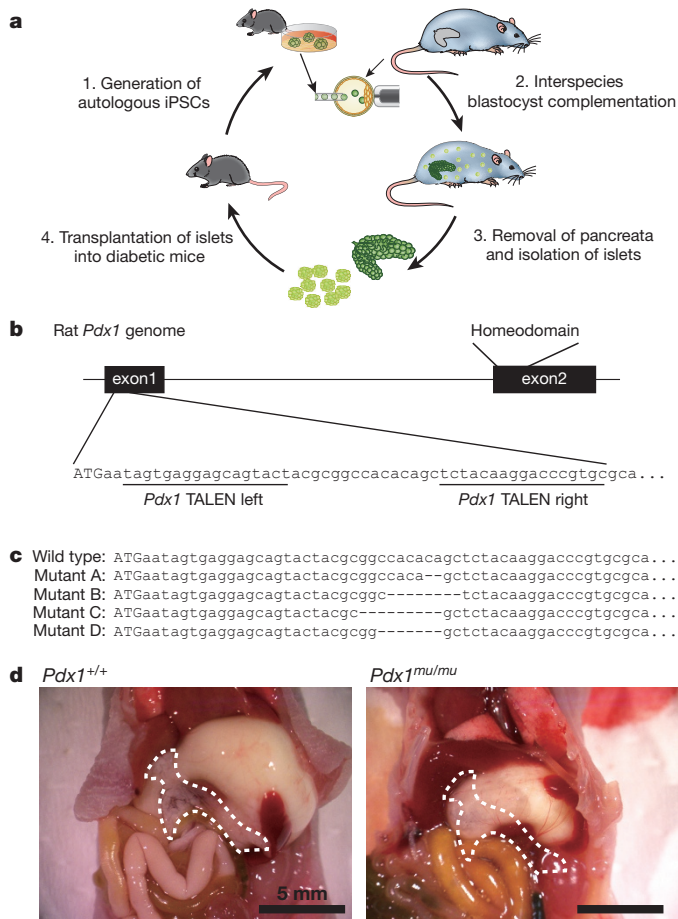


Figure 1 | Generation of apancreatic rats by TALEN-mediated mutagenesis. **a**, Schema of concept for treatment of diabetes by interspecies blastocyst complementation. **b**, Schema of TALEN target site on the rat *Pdx1* genome. Left TALEN was designed 3–17 bp downstream of initiation codon; right TALEN was designed 33–49 bp downstream of initiation codon. The uppercase ‘ATG’ represents the start codon of *Pdx1*. **c**, Variety of mutations found after TALEN injection. **d**, Macroscopic appearance of pancreata (dotted line) in rat. Left, newborn wild-type rat; right, absence of pancreata in age-matched *Pdx1*^{mu/mu} homozygous mutant rat. Scale bars, 0.5 mm.

mRNA are shown in Extended Data Fig. 1c. Both *Pdx1*^{muA} and *Pdx1*^{muB} rats completely lacked a homeodomain, C terminus transactivation domain and nuclear localization signal sequences, as predicted from mouse studies, indicating that they are null mutations^{20,21}.

Some, but not all, adult *Pdx1*^{+ /muA} rats (2 out of 6 rats) and *Pdx1*^{+ /muB} (3 out of 6 rats) showed peak glucose levels of over 387 mg dl⁻¹ (22 mM), or over 200 mg dl⁻¹ at 120 min after glucose administration. This phenotype is consistent with maturity onset diabetes of the young type 4 (MODY 4) in which heterozygous mutation of *PDX1* has been

Table 1 | Generation of apancreatic rats by genome-editing technology

TALEN mRNA concentration (ng μl ⁻¹)	Number of zygotes (%)				Number of offspring (%)	
	Injected	Survived	Cleaved	Transferred	Born	Mutants
3	82	74 (90)	72 (97)	74	41 (55)	2 (5)
	80	75 (94)	75 (100)	75	34 (45)	2 (6)
Total	162	149 (92)	147 (99)	149	75 (50)	4 (5)
10	57	51 (89)	51 (100)	51	20 (39)	2 (10)
	43	36 (84)	32 (89)	36	13 (36)	1 (8)
Total	100	87 (87)	83 (95)	87	33 (38)	3 (9)

Results of introducing mutations into rat *Pdx1* locus by injection of TALEN RNA into zygote.

found^{16,17} (Extended Data Fig. 1b). Cumulatively, these data confirmed that *Pdx1* was the gene responsible for pancreatic organogenesis in rats.

Generation of rat pancreata

To investigate whether *Pdx1*^{mu/mu} rat blastocysts provide a niche that is suitable for pancreatic organogenesis by blastocyst complementation (as seen in the *Pdx1*^{-/-} mouse¹¹), we generated rat pancreata by injecting enhanced green fluorescent protein (EGFP)-labelled wild-type rat embryonic stem cells (rES cells; Wlv3i-1) into blastocysts obtained by crossing mutants A and B. In total, 73 complemented embryos were transferred into surrogate mothers, resulting in 20 live births. Of these 20 pups, 3 (15%) were homozygous *Pdx1*^{mu/mu} and 12 (60%) were heterozygous *Pdx1*^{+ /mu}. All 20 grew and survived normally into adulthood without any disease-specific signs (Fig. 2a). Pancreata from *Pdx1*^{mu/mu} host rats expressed EGFP homogeneously and were similar in size to those of wild-type rats (Fig. 2b). Immunohistochemical (Fig. 2c) and immunofluorescence studies (Fig. 2d, Extended Data Fig. 2a) and

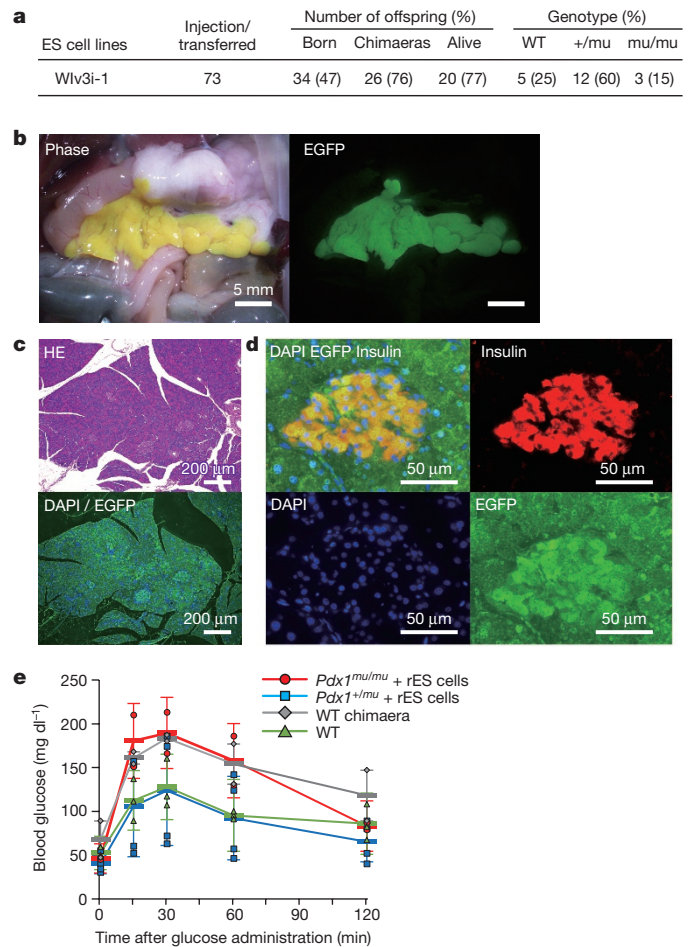


Figure 2 | Generation of rat pancreata by blastocyst complementation.

a, Results of embryo manipulation and genotyping of adult rats. **b**, Macroscopic images at adult stage of rat-PSC-derived pancreata in a *Pdx1*^{mu/mu} chimaera rat (left) and of chimaeric pancreata generated in a *Pdx1*^{+ /mu} rat. Scale bars, 5 mm. **c**, Immunohistochemical appearance of sections of pancreata from a *Pdx1*^{mu/mu} rat. Sections were stained with haematoxylin and eosin (H&E) (upper) and for EGFP and 4',6-diamidino-2-phenylindole (DAPI) (lower). Scale bars, 200 μm. **d**, Immunofluorescence appearance of islets from *Pdx1*^{mu/mu} rat. Sections were stained for EGFP, anti-insulin antibodies and DAPI. Scale bars, 50 μm. **e**, Results of GTTs in *Pdx1*^{mu/mu} ($n = 2$ females), *Pdx1*^{+ /mu} complemented with rat ES cells ($n = 4$; 3 males and 1 female), wild-type chimaera rat (WT chimaera; $n = 2$ males) and wild-type rat (WT; $n = 3$ males). The mean values \pm s.d. were obtained from 2, 3 or 4 independent experiments.

Table 2 | Generation of mPSC-derived pancreata by interspecies blastocyst complementation

Cell lines	Injection/transferred	Number of offspring (%)	Number of offspring (%)			Genotype (%)		
			Born	Chimaeras	Alive	WT	+/ <i>mu</i>	<i>mu/mu</i>
miPSCs	GT3.2	219	149 (68)	74 (50)	63 (63)	23 (37)	34 (54)	6 (10)
mES cells	mRHT	36	23 (64)	11 (48)	5 (45)	3 (60)	-	1 (20)
	SGE2	110	61 (55)	49 (80)	22 (45)	10 (45)	9 (41)	3 (14)

Results of interspecies blastocyst complementation by injection of mPSCs into blastocysts obtained from crossing mutants A and B. mES cells, mouse ES cells; miPSCs, mouse iPSCs.

quantitative analysis of these sections by ImageJ software (Extended Data Fig. 2b) demonstrated that these organs (endocrine and exocrine tissues; islets, acini and duct epithelium) were entirely derived from injected rES cells. We used glucose tolerance tests (GTTs) to examine the functional capacity of pancreata generated. Although blood glucose levels in *Pdx1^{mu/mu}* chimaeric rats were higher than those in *Pdx1^{+/^{mu}}* chimaeric rats and wild-type rats immediately after glucose injection, *Pdx1^{mu/mu}* chimaeric rats recovered normal blood glucose levels (under 200 mg dl⁻¹) 120 min after injection with no significant differences observed between *Pdx1^{mu/mu}* chimaeric rats and wild-type rats (30 min, $P = 0.11$; 120 min, $P = 0.88$). Furthermore, GTT AUC (area under the curve) calculations did not show significant differences (Fig. 2e, Extended Data Fig. 2c). These results demonstrate that *Pdx1^{mu/mu}* rat blastocysts provide a developmental niche amenable to pancreatic organogenesis and that pancreata derived from donor rES cells in this way are both structurally and functionally normal.

Generation of mouse^R pancreata

To generate interspecies chimaeras, EGFP-labelled wild-type mouse induced PSCs (iPSCs) (GT3.2) or mouse ES cells (mRHT, SGE2) were injected into blastocysts obtained by crossing *Pdx1^{+/^{mu}}* founder male rats—in which pancreata arose principally from exogenous rat PSCs—with *Pdx1^{+/^{mu}}* female rats. To determine the genetic backgrounds of liveborn animals produced in this manner, we genotyped EGFP-negative peripheral blood mononuclear cells from 10-week-old pups. The *Pdx1^{mu/mu}* genotype was present in 10% of offspring from the iPSC-injected group and 20% of offspring from the group injected with ES cells (mRHT cells) (Table 2).

Macroscopic observation of pancreata revealed that mouse^R pancreata generated in *Pdx1^{mu/mu}* rats were entirely EGFP-expressing (labelled *Pdx1^{mu/mu}* + mPSCs; Fig. 3a), whereas EGFP expression in mouse^R pancreata generated from *Pdx1^{+/^{mu}}* rats was chimaeric (labelled *Pdx1^{+/^{mu}}* + mPSCs, Fig. 3a). The sizes of mouse^R pancreata generated in *Pdx1^{mu/mu}* rats were close to those of pancreata from age-matched wild-type rats (Fig. 3b): bright-field images of *Pdx1^{mu/mu}* rats at laparotomy demonstrated that, overall, 9 out of 11 mouse^R pancreata were of rat size. Immunohistochemical studies of these pancreata and quantitative analysis of these sections by imageJ software showed almost universal co-expression of EGFP and specific markers of the endocrine and exocrine tissues, that is, islets, acini and duct epithelium (*Pdx1^{mu/mu}* + mPSCs; Fig. 3c, d, Extended Data Fig. 3a, b). These findings indicate normal rat-appropriate differentiation with respect to size and endocrine repertoire.

We then used GTTs to investigate how mouse^R pancreata functioned in their hosts (*Pdx1^{mu/mu}* chimaeric rats). Although *Pdx1^{mu/mu}* chimaeric rats responded more slowly to glucose than did *Pdx1^{+/^{mu}}* chimaeric rats and wild-type rats (60 min, $P = 0.035$ versus wild type; 120 min, $P = 0.025$ versus wild type), the blood glucose level gradually recovered to normal (<200 mg dl⁻¹ at 120 min after glucose administration). Further, GTT AUC calculations did not reveal significant differences (Fig. 3e, Extended Data Fig. 3c). These results indicate that mPSCs can occupy the organogenic niche that is vacant in *Pdx1^{mu/mu}* rat blastocysts, yielding functionally intact mouse pancreata in rats. Although we successfully generated mouse pancreata in all rats, two *Pdx1^{mu/mu}* chimaeric rats developed polyuria and ketonuria consistent with type I diabetes. At 6 weeks of age in one of these rats (rat 186), the fasting blood glucose level was normal (95 mg dl⁻¹) and GTT values were

comparable with those in a *Pdx1^{mu/mu}* chimaeric rat without signs of diabetes (rat 183). However, at 10 weeks of age, the fasting blood glucose level was elevated to 252 mg dl⁻¹ and the response in GTTs was defective (Extended Data Fig. 4a).

The histologic study of pancreata from *Pdx1^{mu/mu}* chimaeric rats with signs of diabetes revealed infiltration of lymphoid cells into the

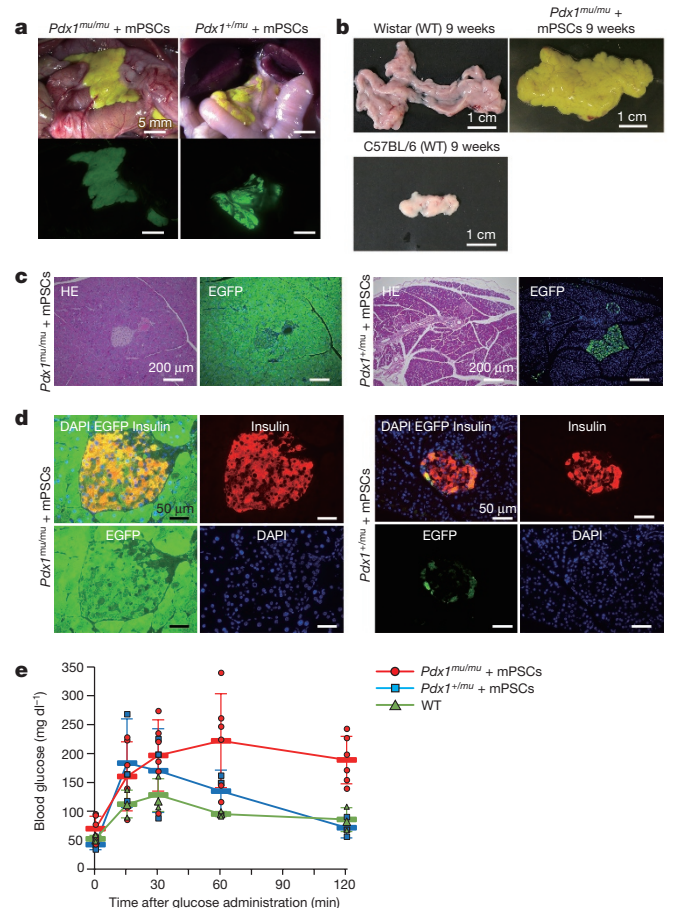


Figure 3 | Generation of mouse pancreata in rat by interspecies blastocyst complementation. **a**, Bright-field images of pancreata in *Pdx1^{mu/mu}* rat generated by blastocyst complementation with mPSCs (upper left) and of *Pdx1^{+/^{mu}}* rat generated by blastocyst complementation with mPSCs (upper right). Fluorescence images of pancreata in *Pdx1^{mu/mu}* chimaeric rat (lower left) and of *Pdx1^{+/^{mu}}* chimaeric rat (lower right). Scale bars, 5 mm. **b**, Bright-field images of pancreata isolated from 9-week-old wild-type Wistar rat (upper left), 9-week-old *Pdx1^{mu/mu}* + mPSCs rat (upper right), and 9-week-old wild-type C57BL/6N mouse. Scale bars, 1 cm. **c**, Immunohistological appearance, sections obtained from pancreata generated in *Pdx1^{mu/mu}* + mPSCs rat (left panel) and in *Pdx1^{+/^{mu}}* + mPSCs rat (right panel). Sections were stained with H&E, EGFP and DAPI. Scale bars, 200 μ m. **d**, Immunofluorescence appearance of islet from *Pdx1^{mu/mu}* + mPSCs rat (left panel) and of *Pdx1^{+/^{mu}}* + mPSCs rat (right panel). Sections were stained with EGFP (lower left), anti-insulin antibodies (lower right) and DAPI (upper right). Scale bars, 50 μ m. **e**, Results of GTTs in *Pdx1^{mu/mu}* + mPSCs rat ($n = 6$; 2 females and 4 males), *Pdx1^{+/^{mu}}* + mPSCs rat ($n = 3$ males) and wild-type rat ($n = 3$ males). The mean values \pm s.d. were obtained from 3 or 6 independent experiments.

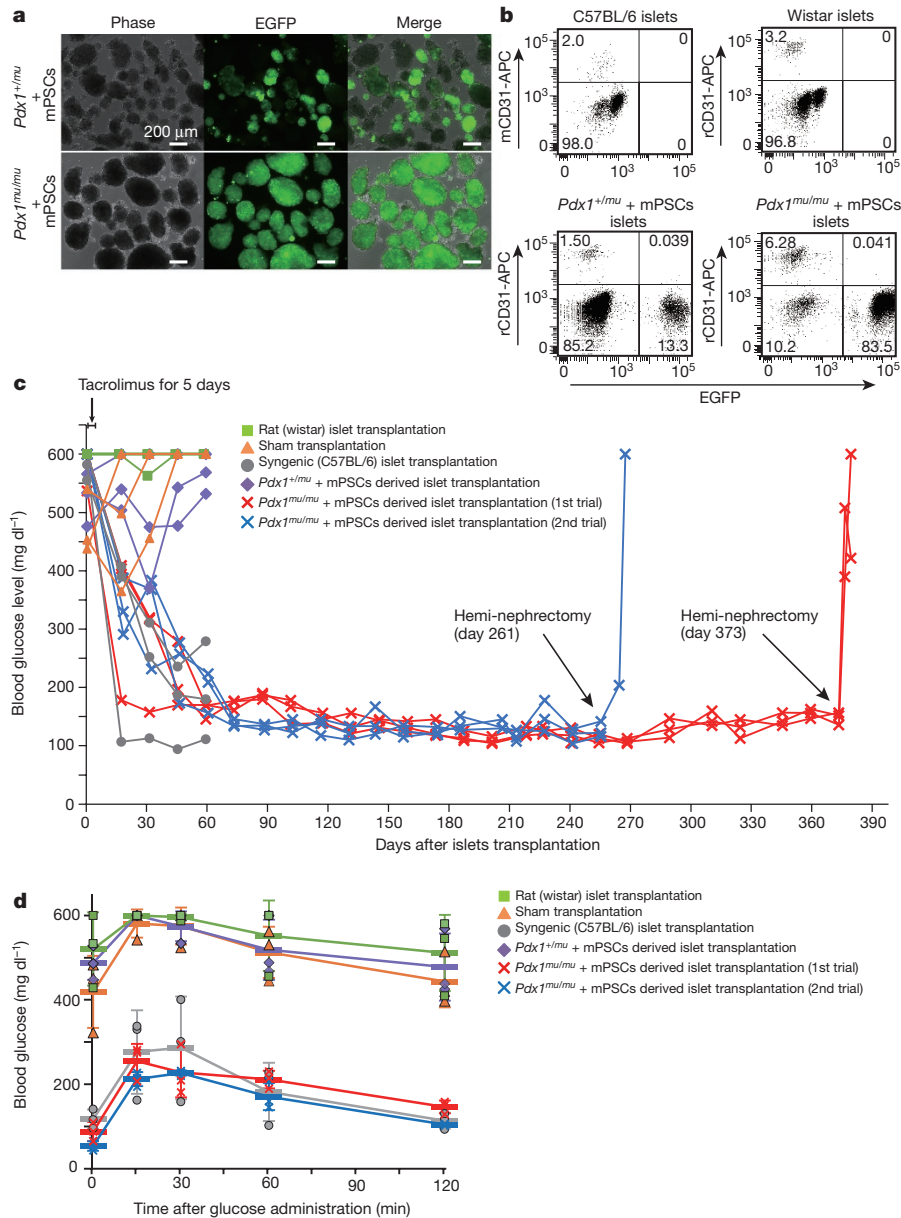


Figure 4 | Transplantation of mouse^R islets into mice with drug-induced diabetes. **a**, Bright-field (left) and fluorescence (middle) images of mouse^R islets isolated from *Pdx1*^{+/mu} (upper) and *Pdx1*^{mu/mu} (lower) rats. Scale bars, 200, μ m. **b**, FACS images, dissociated islet-containing tissues from C57BL/6N mouse (upper left), Wistar rat (upper right), mouse^R in *Pdx1*^{+/mu} rat (lower left), and mouse^R in *Pdx1*^{mu/mu} rat (lower right). Cells were stained with anti-CD31 antibodies. **c**, Blood glucose time course after transplantation of islets into male C57BL/6N mice with STZ-induced diabetes. Each mouse received 100 islets. Arrows indicate time points of administration of anti-inflammatory antibodies and tacrolimus. Nonfasting blood glucose levels were measured weekly for 12 months

pancreata (especially in acinar cells and islets) and islet destruction, consistent with immunologically mediated disease (Extended Data Fig. 4b). These results indicate that type-1-diabetes-like symptoms may gradually develop in *Pdx1*^{mu/mu} rats harbouring mouse^R pancreata, perhaps owing to a breakdown of peripheral tolerance.

Treatment of diabetic mice with mouse^R islets

To examine the therapeutic potential of mouse^R pancreata, isolated pancreatic islets were injected into mice with STZ-induced diabetes. The recipient mice (C57BL/6N; of the same strain from which the mPSCs were used to create pancreata in donor rats by blastocyst

after transplantation. Glucose levels are shown for mice with STZ-induced diabetes transplanted with mouse^R islets taken from *Pdx1*^{mu/mu} host (1st trial, $n = 3$; 2nd trial, $n = 3$), *Pdx1*^{+/mu} host rat ($n = 3$), with islets derived from syngenic strain of host strain (C57BL/6N) as a positive control ($n = 3$), and with islets derived from Wistar rat as a negative control ($n = 3$). Sham transplantation control mice were used as a negative control ($n = 3$). All data were obtained from 3 independent experiments. NC, negative control; PC, positive control. **d**, Results of GTTs 60 days after islet transplantation. The mean values \pm s.d. were obtained from 3 independent experiments.

complementation) were evaluated for recovery of glycaemic control. We collected around 600 islets from 3 *Pdx1*^{mu/mu} chimaeric rats. The islets isolated homogeneously expressed EGFP in tissue sections (Fig. 4a).

However, using fluorescence-activated cell sorting (FACS) of single-cell suspensions prepared from islets, we found that substantial proportions of supporting tissues, including endothelial cells, were of rat origin (Fig. 4b). Therefore, to prevent acute graft rejection, tacrolimus ($0.5 \text{ mg g}^{-1} \text{ d}^{-1}$) and an anti-inflammatory monoclonal antibody (mAb) cocktail ($10 \mu\text{g}$ of each mAb per mouse per day containing anti-mouse interferon- γ mAb, anti-mouse tumour necrosis

factor- α mAb, and anti-mouse IL-1 β mAb) were injected intraperitoneally at implantation and for the first 5 days thereafter. Each diabetic mouse received a single dose of 100 islets placed under the kidney capsule.

Diabetic mice that received mouse^R islets or islets isolated from C57BL/6N mice had normal blood glucose levels for over 370 days without continuous immunosuppression and showed normal responses in GTTs and AUC tests (Figs 4c, d, Extended Data Fig. 7a). When kidneys that contained transplanted islets were removed (on either day 373, trial 1; or day 261, trial 2), blood glucose levels rose substantially, indicating that these 100 transplanted islets were responsible for the regulation of glycaemia (Fig. 4c). By contrast, although blood glucose levels were initially normal in mice that received Wistar rat islets, they became dysregulated after 5 days, probably owing to rejection. Following partial nephrectomy, EGFP-expressing transplanted islets from resected kidneys were identified using fluorescence stereoscopic microscopy (Extended Data Fig. 6a). Immunohistological analysis found that hormone-secreting islet cells (α , β and δ cells) were present, just as with wild-type mouse islets, and that insulin, glucagon and somatostatin were all expressed in the absence of inflammatory cell infiltration (Extended Data Fig. 6b–d). These observations were confirmed by FACS analysis, which also demonstrated the absence of rat supporting tissues such as blood vessels (Extended Data Fig. 6e).

Cumulatively, these data strongly support the hypothesis that pancreatic islets isolated from interspecies blastocyst complementation can be used to achieve long-term glycaemic control.

Discussion

Our work demonstrates that pancreata generated in a xenogeneic environment by interspecies blastocyst complementation are functional and rescue the lethal phenotype of Pdx1-deficient rats. Mouse^R islets isolated from these pancreata and engrafted beneath the renal capsule of syngeneic mice with STZ-induced diabetes normalized blood glucose levels for a prolonged period without immunosuppression.

Current challenges of islet cell transplantation, such as shortage of donor pancreata, difficulty in long-term maintenance of blood glucose levels, and side effects of immunosuppression, could potentially be addressed through generation of pancreata from patient-specific iPSCs. Of particular interest in our iPSC approach, the time course observed for restoration of glycaemic control by mouse^R islets and by primary controls (islets from adult mice of the genetic background of the recipient mice) was nearly identical. This indicates that the pancreata generated through blastocyst complementation probably underwent near-normal differentiation with proper epigenetic changes, leading to generation of fully functional endocrine, as well as exocrine cells. Indeed, islets generated by blastocyst complementation contained all endocrine cells— α , β and δ —in similar ratios to wild-type islets. This is probably the reason for the precise regulation of blood glucose levels observed in our study²². Furthermore, the blastocyst complementation system excludes the possibility of teratoma development through contamination of undifferentiated PSCs. For these reasons, the system described here appears to be superior to the previously reported system, which uses PSC-derived islets generated *in vitro*²³.

Several concerns regarding organ generation through blastocyst complementation remain, including contamination of donor organs by residual cells from a different species. However, these concerns must be considered in the context of previous data that report long-term engraftment for allogeneic islets to be far poorer than that for autologous islets²⁴ and that 50%–70% of islets are destroyed by hyperacute rejection immediately after xenotransplantation²⁵. We did not, however, observe any such negative effects in our experiments. Our immunosuppression regime was stopped after only 5 days, which appears to have allowed enough time for the host (mouse) immune system to eliminate residual donor (rat) cells without triggering a hyperacute response. These data therefore provide proof-of-principle for the treatment of type 1 diabetes using islets harvested from organs generated using blastocyst complementation with donor iPSCs.

Not only does this *in vivo* engineering approach permit recapitulation of the complex cell–organ interactions and epigenetic changes of physiological intrauterine development, it also provides a novel route to investigate broader biological questions, such as regulation of organ size in development and disease. For example, we noted that pancreata generated from mPSCs injected into rat blastocysts were of rat size, not of mouse or intermediate size, whereas rat-PSC-derived pancreata generated in mouse were of mouse size¹¹. Although pancreata size determination has to date been ascribed to cell-intrinsic properties such as the number of embryonic progenitor cells²⁶, our observations suggest that extrinsic factors also contribute, with cross-talk between extrinsic and intrinsic factors probably converging on key signalling pathways such as Hippo^{27–29}. If this were confirmed, greater understanding of these pathways could open up novel therapeutic opportunities for organ rescue through promotion of endogenous regeneration or inhibition of uncontrolled growth within the context of cancer.

With respect to a more direct clinical translation of interspecies blastocyst complementation in patients, this approach will require organ generation in animals closer to humans in size or in evolutionary distance such as sheep, pigs or non-human primates. As suggested by our study, islets generated in this manner appear functionally and immunologically identical to primary host islets. Generation of human islets in this manner will enable direct comparison between such islets and islets generated through ‘standard’ *in vitro* directed differentiation and/or tissue-engineering approaches^{15,30} in achieving clinically important therapeutic endpoints. This observation therefore provides part of the scientific justification for addressing the reasonable and as-yet unresolved ethical concerns surrounding use of this technology. We propose that further studies in this field are both urgently needed and fully warranted.

Online Content Methods, along with any additional Extended Data display items and Source Data, are available in the online version of the paper; references unique to these sections appear only in the online paper.

Received 4 June; accepted 21 December 2016.

Published online 25 January 2017.

- Pagliuca, F. W. *et al.* Generation of functional human pancreatic β cells *in vitro*. *Cell* **159**, 428–439 (2014).
- Yusa, K. *et al.* Targeted gene correction of α 1-antitrypsin deficiency in induced pluripotent stem cells. *Nature* **478**, 391–394 (2011).
- Shi, Y., Kirwan, P., Smith, J., Robinson, H. P. C. & Livesey, F. J. Human cerebral cortex development from pluripotent stem cells to functional excitatory synapses. *Nat. Neurosci.* **15**, 477–486 (2012).
- Nakamura, S. *et al.* Expandable megakaryocyte cell lines enable clinically applicable generation of platelets from human induced pluripotent stem cells. *Cell Stem Cell* **14**, 535–548 (2014).
- Sun, N. *et al.* Patient-specific induced pluripotent stem cells as a model for familial dilated cardiomyopathy. *Sci. Transl. Med.* **4**, 130ra47 (2012).
- Völkner, M. *et al.* Retinal organoids from pluripotent stem cells efficiently recapitulate retinogenesis. *Stem Cell Rep.* **6**, 525–538 (2016).
- Lancaster, M. A. *et al.* Cerebral organoids model human brain development and microcephaly. *Nature* **501**, 373–379 (2013).
- Spence, J. R. *et al.* Directed differentiation of human pluripotent stem cells into intestinal tissue *in vitro*. *Nature* **470**, 105–109 (2011).
- Takebe, T. *et al.* Vascularized and functional human liver from an iPSC-derived organ bud transplant. *Nature* **499**, 481–484 (2013).
- Takasato, M. *et al.* Directing human embryonic stem cell differentiation towards a renal lineage generates a self-organizing kidney. *Nat. Cell Biol.* **16**, 118–126 (2014).
- Kobayashi, T. *et al.* Generation of rat pancreas in mouse by interspecific blastocyst injection of pluripotent stem cells. *Cell* **142**, 787–799 (2010).
- Rashid, T., Kobayashi, T. & Nakauchi, H. Revisiting the flight of Icarus: making human organs from PSCs with large animal chimeras. *Cell Stem Cell* **15**, 406–409 (2014).
- Shapiro, A. M. J. *et al.* International trial of the Edmonton protocol for islet transplantation. *N. Engl. J. Med.* **355**, 1318–1330 (2006).
- Rezania, A. *et al.* Reversal of diabetes with insulin-producing cells derived *in vitro* from human pluripotent stem cells. *Nat. Biotechnol.* **32**, 1121–1133 (2014).
- Vegas, A. J. *et al.* Long-term glycaemic control using polymer-encapsulated human stem cell-derived β cells in immune-competent mice. *Nat. Med.* **22**, 306–311 (2016).
- Stoffers, D. A., Ferrer, J., Clarke, W. L. & Habener, J. F. Early-onset type-II diabetes mellitus (MODY4) linked to IPF1. *Nat. Genet.* **17**, 138–139 (1997).

17. Ahlgren, U., Jonsson, J., Jonsson, L., Simu, K. & Edlund, H. β -cell-specific inactivation of the mouse *lpl1/Pdx1* gene results in loss of the β -cell phenotype and maturity onset diabetes. *Genes Dev.* **12**, 1763–1768 (1998).
18. Takahashi, R., Hirabayashi, M. & Ueda, M. Production of transgenic rats using cryopreserved pronuclear-stage zygotes. *Transgenic Res.* **8**, 397–400 (1999).
19. Grau, J., Boch, J. & Posch, S. TALENoffer: genome-wide TALEN off-target prediction. *Bioinformatics* **29**, 2931–2932 (2013).
20. Oliver-Krasinski, J. M. *et al.* The diabetes gene *Pdx1* regulates the transcriptional network of pancreatic endocrine progenitor cells in mice. *J. Clin. Invest.* **119**, 1888–1898 (2009).
21. Moede, T., Leibiger, B., Pour, H. G., Berggren, P. & Leibiger, I. B. Identification of a nuclear localization signal, RRMKWKK, in the homeodomain transcription factor PDX-1. *FEBS Lett.* **461**, 229–234 (1999).
22. Rodriguez-Diaz, R. *et al.* α cells secrete acetylcholine as a non-neuronal paracrine signal priming beta cell function in humans. *Nat. Med.* **17**, 888–892 (2011).
23. Balboa, D. & Otonkoski, T. Human pluripotent stem cell based islet models for diabetes research. *Best Pract. Res. Clin. Endocrinol. Metab.* **29**, 899–909 (2015).
24. Sutherland, D. E. R. *et al.* Islet autotransplant outcomes after total pancreatectomy: a contrast to islet allograft outcomes. *Transplantation* **86**, 1799–1802 (2008).
25. Bennet, W. *et al.* Incompatibility between human blood and isolated islets of Langerhans: a finding with implications for clinical intraportal islet transplantation? *Diabetes* **48**, 1907–1914 (1999).
26. Stanger, B. Z., Tanaka, A. J. & Melton, D. A. Organ size is limited by the number of embryonic progenitor cells in the pancreas but not the liver. *Nature* **445**, 886–891 (2007).
27. Camargo, F. D. *et al.* YAP1 increases organ size and expands undifferentiated progenitor cells. *Curr. Biol.* **17**, 2054–2060 (2007).
28. Yimlamai, D. *et al.* Hippo pathway activity influences liver cell fate. *Cell* **157**, 1324–1338 (2014).
29. Barry, E. R. *et al.* Restriction of intestinal stem cell expansion and the regenerative response by YAP. *Nature* **493**, 106–110 (2013).
30. Agulnick, A. D. *et al.* Insulin-producing endocrine cells differentiated *in vitro* from human embryonic stem cells function in macroencapsulation devices *in vivo*. *Stem Cells Transl. Med.* **4**, 1214–1222 (2015).

Acknowledgements We thank A. Oshima and H. Tsukui for technical support, K. Okada for secretarial support, H. Nagashima and M. Watanabe for advice in preparing the manuscript, A. S. Knisely for reading of the manuscript and Japan Insulin-Dependent Diabetes Mellitus (IDDM) Network for continuous support. This work was supported by grants from Japan Science and Technology Agency, Exploratory Research for Advanced Technology, Leading Advanced Projects for medical innovation, Japan Agency for Medical Research and Development, Japan Society for the Promotion of Science, KAKENHI Grant Number 26460358, research grant for type 1 diabetes, Japan IDDM Network and California Institute for Regenerative Medicine.

Author Contributions T.Y. and H.S. designed, performed, and analysed all experiments and wrote the manuscript. M.I.-K., T.G., H.H., M.S., T.K., A.Y., and A.U. performed embryo manipulation. N.M. performed data analysis. Y.O. performed histopathological analysis. S.H. performed establishment of iPSCs. H.M. performed data analysis. D.T.R. wrote the manuscript. M.H. performed embryo manipulation and data analysis. H.N. designed the study and wrote the manuscript.

Author Information Reprints and permissions information is available at www.nature.com/reprints. The authors declare competing financial interests: details are available in the online version of the paper. Readers are welcome to comment on the online version of the paper. Correspondence and requests for materials should be addressed to H.N. (nakauchi@stanford.edu).

Reviewer Information *Nature* thanks H. Lickert, Q. Zhou and the other anonymous reviewer(s) for their contribution to the peer review of this work.

METHODS

Animals. C57BL/6N mice, ICR mice and Wistar rats were purchased from SLIC Japan (Shizuoka, Japan). All animals were maintained under specific pathogen-free conditions. All animal experiments were approved by the Institutional Animal Care and Use Committee, and performed in accordance with the guidelines of the University of Tokyo and the National Institute for Physiological Sciences. Diabetes was induced in 8-week-old C57BL/6N male mice by intravenous injection of 150 mg kg⁻¹ of STZ. Mice with nonfasting blood glucose levels over 350 mg dl⁻¹ 1 week after STZ administration were used. Embryo culture and manipulation are described¹¹.

Islet isolation and transplantation. Rodent islets conventionally are isolated by collagenase perfusion of the pancreata through the common bile duct. However, the pancreata of *Pdx1^{mu/mu}* chimaeric rats could not be perfused in this way because the pancreaticobiliary junction was maldeveloped in all (Extended Data Fig. 5). Therefore, we isolated islets by digestion of minced pancreata with collagenase. Pancreata removed from interspecific chimaera were inflated by interstitial injection of Gey's balanced salt solution (GBSS; Sigma-Aldrich). GBSS-filled pancreata were minced using scissors. Small pieces of chopped pancreata were digested with collagenase XI (Sigma-Aldrich) to release islets from exocrine tissue. After 6–8 min incubation, islets were picked up using glass micropipettes and transplanted beneath the kidney capsule of 10-week-old male mice with STZ-induced diabetes, as previously described¹¹. To prevent acute graft rejection, 0.5 mg per g (body weight) per day of tacrolimus, was injected intraperitoneally on the day of transplantation and on each of the following 4 days, in addition to an anti-inflammatory cocktail (all components, Affymetrix) containing anti-mouse interferon- γ mAb (rat IgG κ , 16-7312, clone R4-6A2), anti-mouse tumour necrosis factor- α mAb (rat IgG1 κ , 16-7322, clone MP6-XT3) and anti-mouse IL-1 β (hamster IgG, 16-7012, clone B122).

Microinjection of TALENs mRNA. The mRNA of TALENs (left and right) and rat Exo1 were generated by *in vitro* transcription. Linearized plasmids were transcribed from T7 promoter using mMESSAGING mMACHINE T7 ULTRA Transcription Kit (Thermo Fisher Scientific) and resultant mRNAs were cleaned up by MEGAclear Kit (Thermo Fisher Scientific). 3 or 10 ng μ l⁻¹ of each mRNA was prepared by dilution in RNase-free-water and mixture of right TALEN, left TALEN and Exo1 were injected into the male pronuclei of zygotes by microinjection, as previously reported¹⁸.

TALEN potential off-target sites were predicted by TALENoff software. We chose 21 candidates (5 in exonic loci, 13 in intronic loci, 3 in intergenic loci) from TOP200 candidates¹⁹. We performed PCR amplification of genomic DNA from *Pdx1^{+/muA}*, *Pdx1^{+/muB}* and wild-type Wistar rats, subjecting the amplicons to Sanger sequencing.

Genotyping of chimaeric rats. Genomic DNA was isolated from fluorescent-marker-negative cells isolated by FACS from chimaeric-rat blood samples.

The TALEN target region of *Pdx1* was amplified by PCR using the following primers: (forward) 5'-GCTGAGAGTCCGTGAGCTGCCAG-3' and (reverse) 5'-GGAACGCTTAAAGATCGTAGCAGC-3'. The PCR products were sequenced. Total RNA was isolated from duodenum of *Pdx1^{muA/muB}* mice and reverse-transcribed by Superscript III reverse transcriptase (Thermo Fisher Scientific) with oligodT primer. *Pdx1^{muA}* or *Pdx1^{muB}* full-length cDNA were amplified by PCR using the following primers: (forward) 5'-GGCGCTGAGAGTCCGTGAGCTGC-3' and (reverse) 5'-TTTTTTTTTTTTTTTGAACCTCAAACAG-3'.

Monitoring blood glucose levels. Nonfasting blood glucose levels were determined (Medisafe-Mini glucometer; Terumo) weekly after islet transplantation. GTTs in overnight-fasted chimaera rats was conducted 0, 15, 30, 60 and 120 min after intraperitoneal injection of glucose (50% D-glucose solution, 2.5 g per kg body weight). Tail-vein blood was sampled by phlebotomy.

Non-fasting serum mouse or rat c-peptide levels were analysed by enzyme-linked immunosorbent assay (ELISA) (mouse c-peptide ELISA kit, Shibayagi and Morinaga Institute of Biological Science; rat c-peptide ELISA kit, MERCODIA AB). Serum was isolated from 10-week-old *Pdx1^{muA/muB}* + mPSCs chimaeras, C57BL/6N mice and Wistar rats. Serum was obtained from STZ-treated diabetic mice transplanted with mouse^R islets 260 or 372 days after transplantation.

Cell culture. SGE2 (EGFP-expressing mES cells) were derived from blastocysts generated from mating C57BL/6N female mice with C57BL/6N-Tg male mice (CAG-EGFP) (SLC Japan). mRHT (mES cells) were derived from blastocysts generated from mating male and female H2B-tdTomato knock-in mice with human histone H2B and tdTomato fusion gene in the mouse ROSA locus (T.K., unpublished data). Wlv3i-1 (rES cells) and GT3.2 (miPSCs) have been previously described^{11,31}.

Maintenance of mPSCs and rPSCs has been previously described^{32,33}. Briefly, mPSCs were cultured on mitomycin-C-treated mouse embryonic fibroblasts in Dulbecco's modified Eagle's medium supplemented with 10% fetal bovine serum, 0.1 mM 2-mercaptoethanol, 0.1 mM nonessential amino acids, 1 mM sodium pyruvate, and 1,000 units per ml of mouse leukaemia inhibitory factor (all Thermo Fisher Scientific) and 1% L-glutamine-penicillin-streptomycin (Sigma-Aldrich). rPSCs were cultured on mitomycin-C-treated mouse embryonic fibroblasts in N2B27 medium supplemented with 1 μ M mitogen-activated protein kinase inhibitor PD0325901 and 3 μ M glycogen synthase kinase inhibitor CHIR99021 (both Axon Groeningen). All PSC lines were authenticated by chimaera formation. These cell lines were not contaminated with mycoplasma.

Immunohistochemistry. Isolated pancreata and islets were fixed in 4% paraformaldehyde in phosphate-buffered saline solution (PBS). Paraffin-embedded sections were incubated with blocking buffer (Active Motif) for 1 h at room temperature. The sections were incubated with primary antibodies, diluted in blocking buffer for 1 h at room temperature, and washed three times with PBS. They were then incubated with secondary antibodies for 1 h at room temperature. Primary antibodies used were guinea pig anti-insulin (Abcam; ab7842), rabbit anti-glucagon (Nichirei Bioscience, 422271), rabbit anti-somatostatin (Nichirei Bioscience 422651), rabbit anti-cytokeratin 19 (Abcam; ab52625, clone EP1580Y), mouse anti-amylase (SantaCruz; SC-46657, clone G-10) and goat anti-GFP (Abcam; ab6673), with Alexa-488-, Alexa-546-, and Alexa-633-conjugated secondary antibodies (Thermo Fisher Scientific). After antibody treatment, sections were mounted with Vectashield (Vector Laboratories), a mounting medium containing DAPI (Thermo Fisher Scientific) for nuclear counterstaining, and sections were observed under fluorescence microscopy. Three to five sections per slide were imaged and processed using Image J. For detection of lymphoid infiltration, DAB immunohistochemistry was performed with rabbit anti-CD3 (Abcam; ab5690) and rabbit anti-CD11b (Bioss Inc.; bs-1014R).

Flow cytometry studies. Islets or small pieces of kidney that included transplanted islets were dispersed into single cells with collagenase type1A (Sigma-Aldrich). Dispersed cells stained with phycoerythrin (PE)-conjugated anti-mouse CD31 (Thermo Fisher Scientific; A16201, clone 390) or allophycocyanin (APC)-conjugated anti-rat CD31 (Thermo Fisher Scientific; 50-0310-82, clone TLD-3A12) were subjected to FACS CantoII analysing (BD Biosciences). Data were collected for all of the dispersed cells and analysed.

Statistics and reproducibility. The experiments were not randomized and the investigators were not blinded to allocation during experiments and outcome assessment. Sample size was estimated on the basis of previous publications. Statistical significance was calculated by *F*-test and Student's *t*-test (compare two groups) and the similarity to the Mendelian ratio was analysed by chi-square test (with Excel and Graphpad Prism software). *P* < 0.05 was considered to be statistically significant. Data are presented as mean \pm s.d. Immunohistochemistry and flow-cytometry studies were repeated three times independently with similar results.

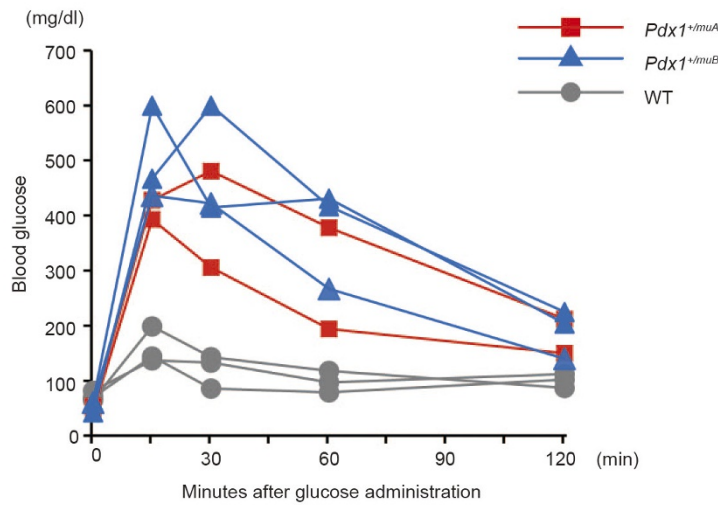
Data availability. All relevant data that are included with this study are available from corresponding author upon reasonable request.

- Hirabayashi, M. *et al.* Ability of tetraploid rat blastocysts to support fetal development after complementation with embryonic stem cells. *Mol. Reprod. Dev.* **79**, 402–412 (2012).
- Yamaguchi, T. *et al.* Development of an all-in-one inducible lentiviral vector for gene specific analysis of reprogramming. *PLoS One* **7**, e41007 (2012).
- Yamaguchi, T., Hamanaka, S. & Nakauchi, H. The generation and maintenance of rat induced pluripotent stem cells. *Methods Mol. Biol.* **1210**, 143–150 (2014).

a

	Number of offspring				Total offspring
	Wild type	<i>Pdx1</i> ^{+/<i>muA</i>}	<i>Pdx1</i> ^{+/<i>muB</i>}	<i>Pdx1</i> ^{<i>muA/muB</i>} (Apancreatic)	
<i>Pdx1</i> ^{+/<i>muA</i>} × <i>Pdx1</i> ^{+/<i>muB</i>} (Trial #1)	1	4	3	4 (4)	12
<i>Pdx1</i> ^{+/<i>muA</i>} × <i>Pdx1</i> ^{+/<i>muB</i>} (Trial #2)	3	5	4	2 (2)	14
<i>Pdx1</i> ^{+/<i>muA</i>} × <i>Pdx1</i> ^{+/<i>muB</i>} (Trial #3)	2	2	4	2 (2)	10
Total	6	11	11	8 (8)	36
Expected mendelian frequencies	9	9	9	9	

b

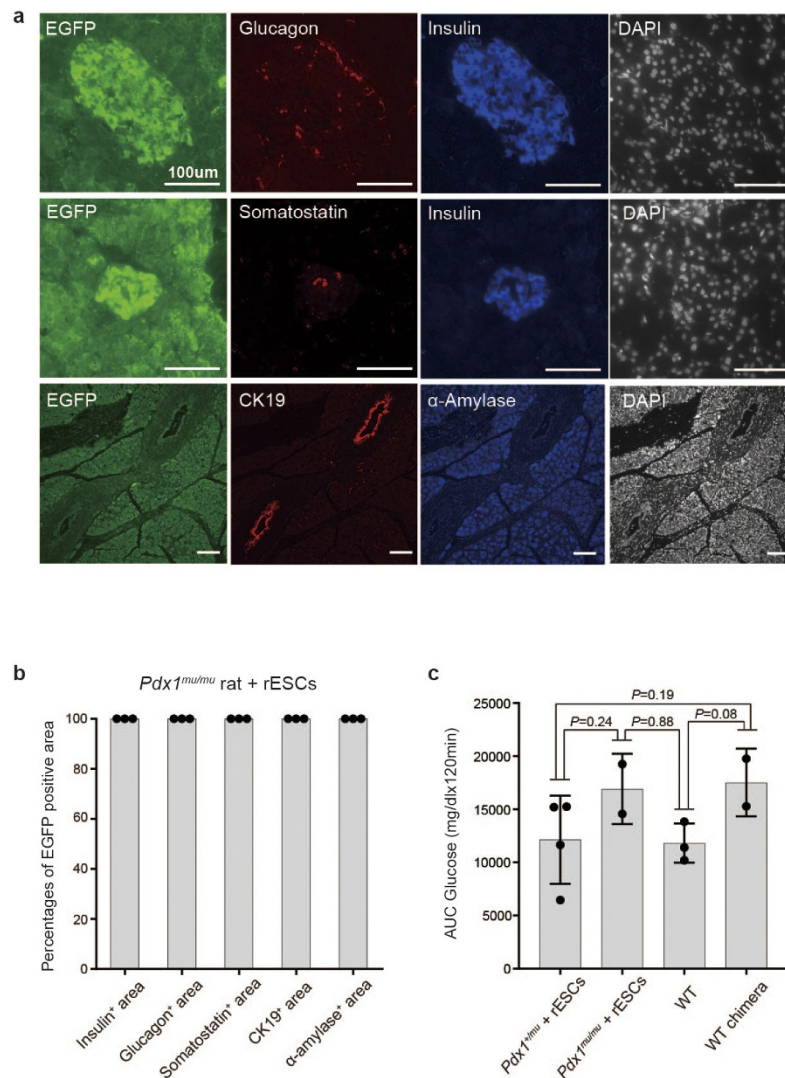


c

Pdx1^{*muA*}: MNSEEQYYAATALQGVPVRIPEGSGARVQC*
Pdx1^{*muB*}: MNSEEQYYAALQGVPVRIPEGSGARVQC*
Pdx1^{*wt*}: MNSEEQYYAATQLYKDFCAFQRFVPEFSANPPACLVMGRQPPPPPTQFAGSLGTLEQQ
 SPPDISPYEVPPLADDPAGAHLHHHLPAQLGLAHPPPGPPFNGTETGGLEEPSRVHLFFP
 WMKSTKAHAWKSQWAGGAYAAEPEENKTRTAYTRAQLELEKEFLFNKYISRPRVELA
 VMLNLTERHIKIWFQNRMKWKEEDKRSSTSGGGGEEPEQCAVTSGEELLALPK
 PPPPGVVPVSGVPAAREGRLPSGLSASPQFSSIAPLRPQEPR*

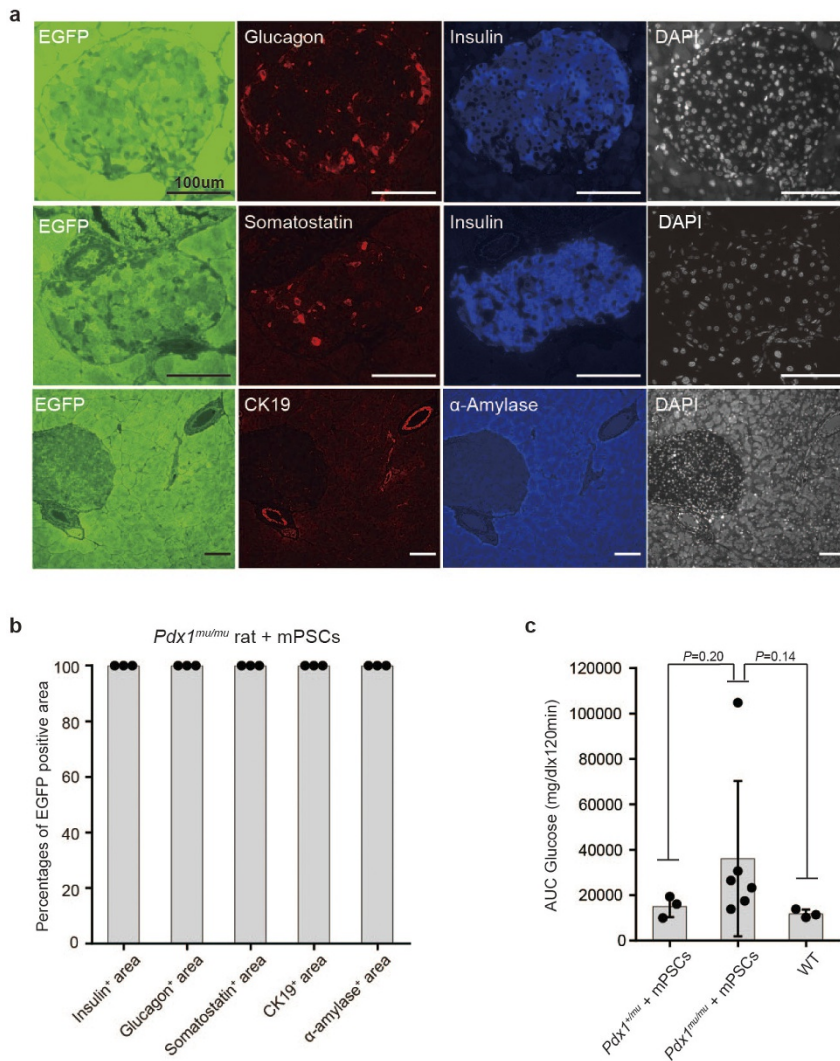
Extended Data Figure 1 | The birth rate of *Pdx1*^{*mu/mu*} rats and phenotype of *Pdx1*^{+/*mu*} rats. a, Results of mating *Pdx1*^{+/*muA*} with *Pdx1*^{+/*muB*}. Wild-type, *Pdx1*^{+/*mu*} and *Pdx1*^{*mu/mu*} rats were born in the mendelian ratio ($X^2 = 2$, $P = 0.37$ by chi-squared test). b, Results of GTTs in *Pdx1*^{+/*mu*}. MODY-like hyper-glycaemia were observed in *Pdx1*^{+/*muA*}

(2 of 6 rats) and *Pdx1*^{+/*muB*} (3 of 6 rats). c, Amino acid sequences of *Pdx1*^{*muA*}, *Pdx1*^{*muB*} and wild-type *Pdx1*, which are predicted from full-length cDNA derived from mRNA in duodenum of *Pdx1*^{*muA/muB*} or *Pdx1*^{+/*+*} rats.



Extended Data Figure 2 | Immunofluorescence photomicrographs of rES-cell-derived pancreata generated in *Pdx1^{mu/mu}* chimaeric rats. **a**, Pancreata sections were stained with antibodies against rat glucagon, rat insulin, rat somatostatin, rat CK19 and rat α -amylase. Scale bars, 100 μ m. **b**, Quantitative analysis of sections of pancreata. Percentages of EGFP-expressing areas in areas that were positive for insulin, glucagon, somatostatin, CK19 or α -amylase were analysed by image J software

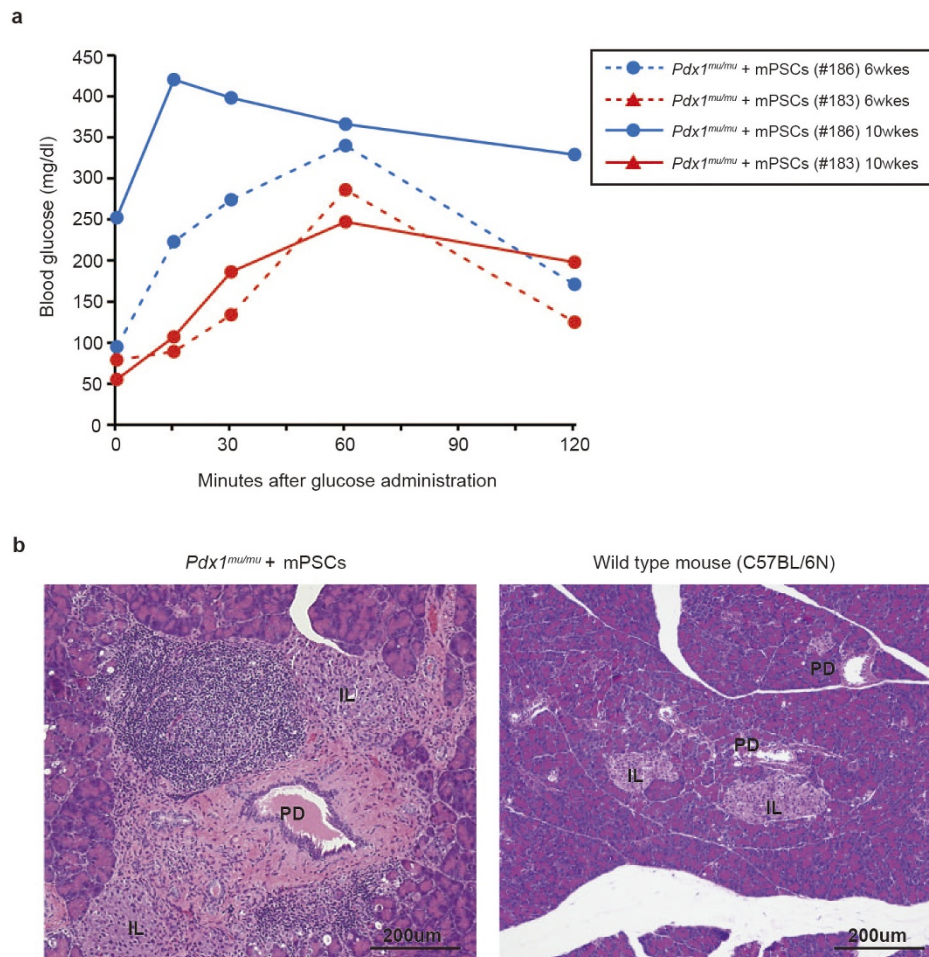
($n = 3$). The mean values \pm s.d. were obtained from 3 biological replicates. **c**, The area under glucose curve (AUC glucose), calculated from GTT data in Fig. 2e. The mean values \pm s.d. were obtained from 2 (*Pdx1^{mu/mu}* + rES cells, WT chimaera), 3 (WT), or 4 (*Pdx1^{+/mu}* + rES cells) independent experiments ($P = 0.24$ *Pdx1^{+/mu}* + rESCs versus *Pdx1^{mu/mu}* + rESCs; $P = 0.88$ *Pdx1^{mu/mu}* + rESCs versus WT; $P = 0.08$ WT chimaera versus WT; $P = 0.19$ WT chimaera versus *Pdx1^{+/mu}* + rESCs; Student's *t*-test).



Extended Data Figure 3 | Immunofluorescence photomicrographs of miPSC-derived-pancreata generated in *Pdx1^{mu/mu}* chimaeric rats.

a, Pancreata sections were stained with antibodies against mouse glucagon, mouse insulin, mouse somatostatin, mouse CK19 and mouse α -amylase. Scale bars, 100 μ m. **b**, Quantitative analysis of sections of pancreata. Percentages of EGFP-expressing areas in areas that were positive for insulin, glucagon, somatostatin, CK19 or α -amylase were analysed by Image J

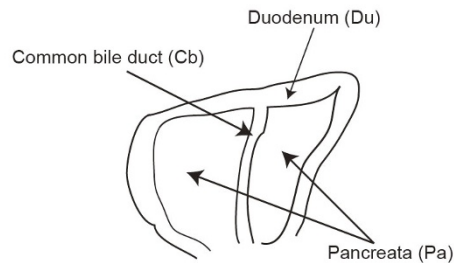
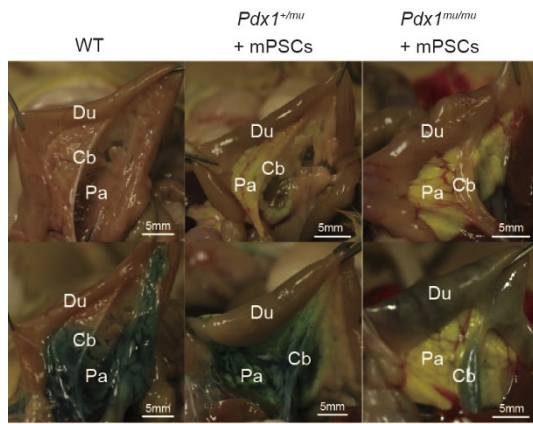
software ($n = 3$). The mean values \pm s.d. were obtained from 3 biological replicates. **c**, AUC glucose, calculated from GTT data in Fig. 3e. The mean values \pm s.d. were obtained from 3 (*Pdx1^{+/-mu}* + mPSCs; WT), or 6 (*Pdx1^{mu/mu}* + mPSCs) independent experiments ($P = 0.20$ *Pdx1^{+/-mu}* + mPSCs versus *Pdx1^{mu/mu}* + mPSCs; $P = 0.14$ *Pdx1^{mu/mu}* + mPSCs versus WT; Student's *t*-test).



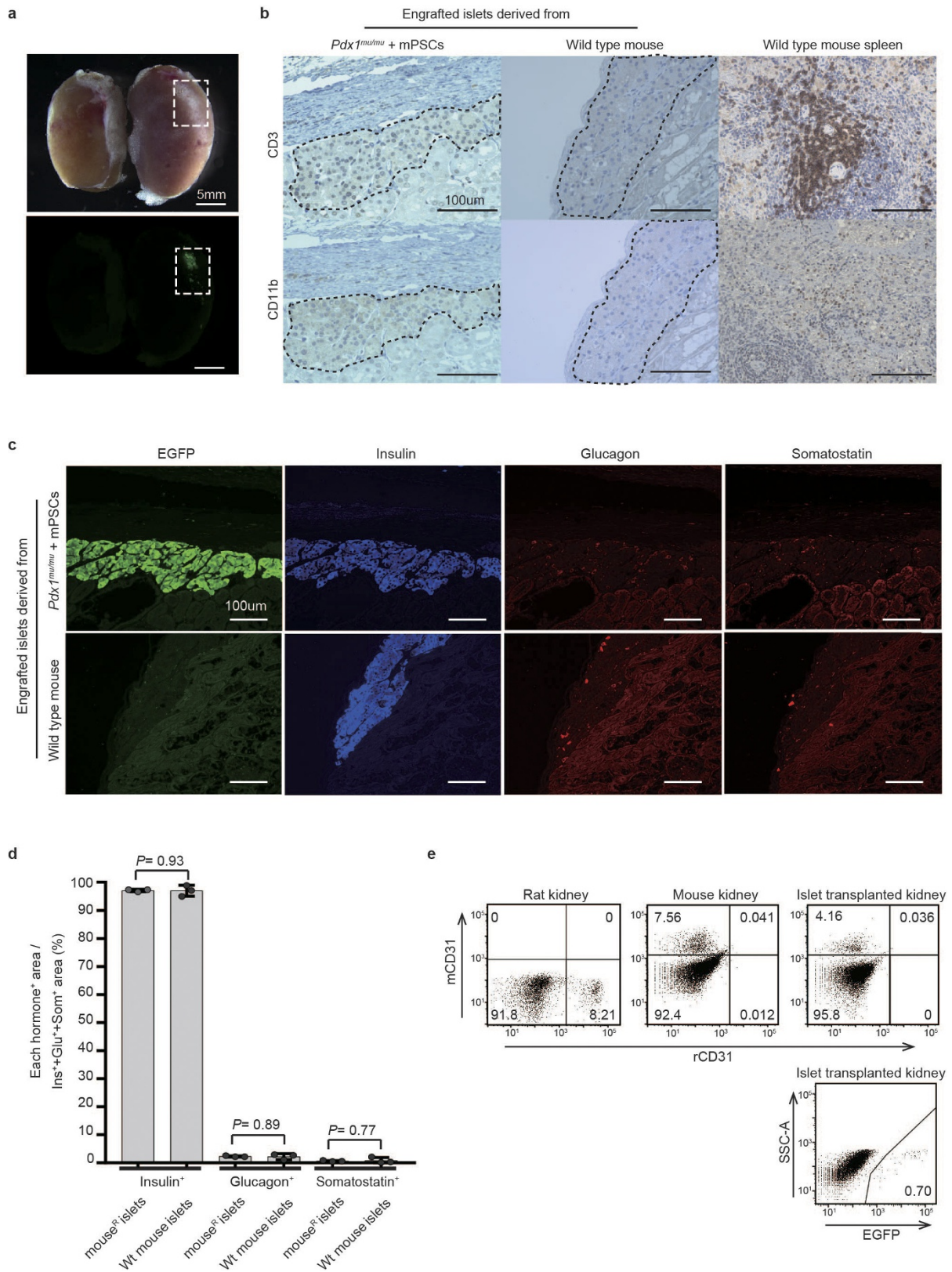
Extended Data Figure 4 | Clinical biochemistry and histologic observations in *Pdx1*^{mut/mut} chimeric rat with diabetic-like symptoms.

a, GTTs results, 6 weeks and 10 weeks after birth, in *Pdx1*^{mut/mut} chimeric rats that possess mPSC-derived pancreata (chimaeras 183 and 186). Blood

sampling at the same time points as in Fig. 3e. Chimaera 186 showed diabetic-like symptoms. **b**, Photomicrographs of pancreata of *Pdx1*^{mut/mut} chimeric rat (chimaera 186) (left) and C57BL/6N mouse pancreata (right). IL, islet of Langerhans; PD, pancreatic duct.

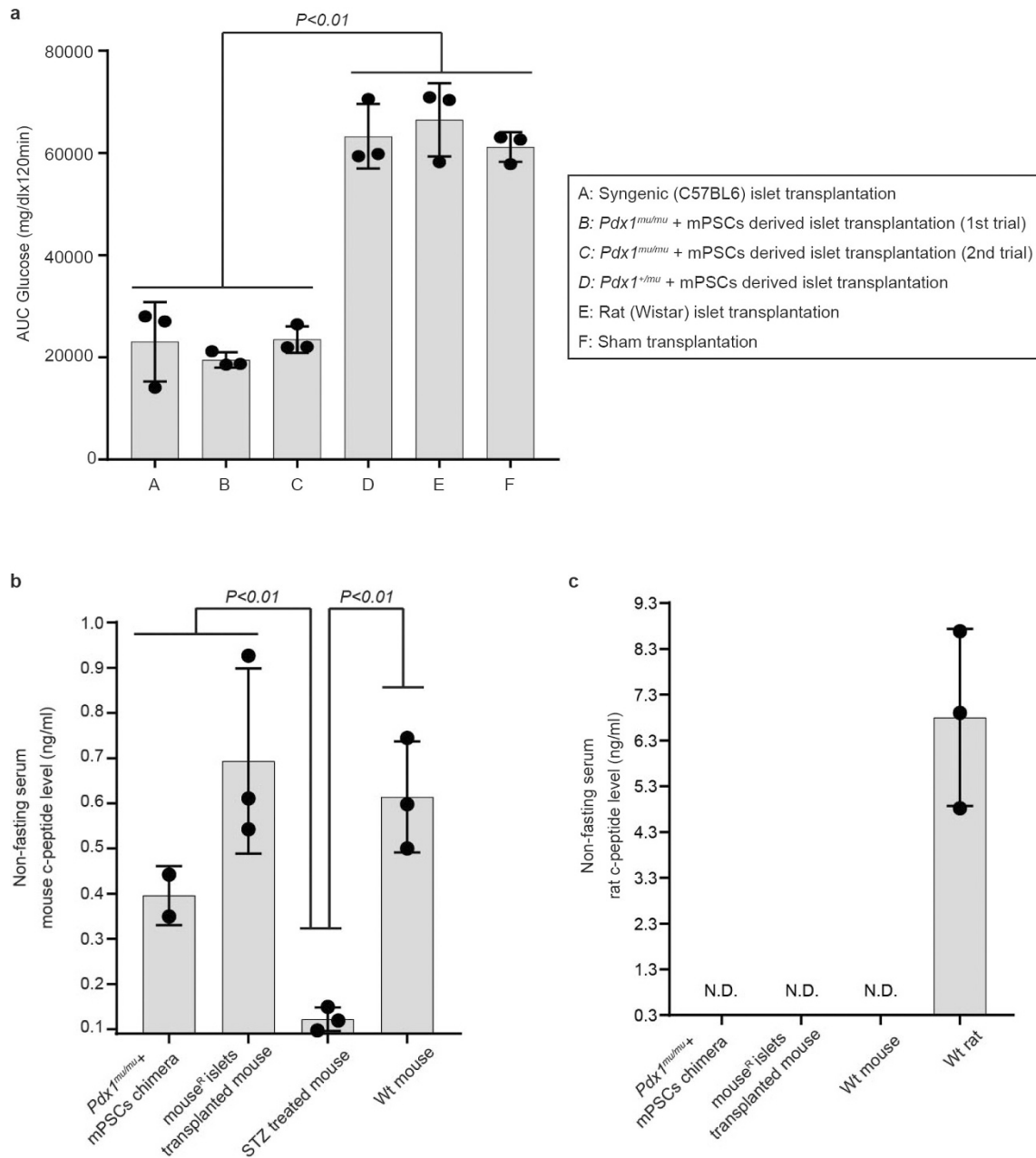


Extended Data Figure 5 | Injection studies of pancreatic duct through common bile duct. PBS-containing trypan blue was injected from the duodenum into the common bile duct (see diagram, bottom) of a wild-type Wistar rat (upper left, before injection; lower left, after injection), *Pdx1*^{+/*mu*} chimaeric rat (upper middle, before injection; lower middle, after injection), and a *Pdx1*^{*mu*/*mu*} chimaeric rat (upper right, before injection; lower right, after injection). PBS diffused throughout the pancreata in wild-type rat and *Pdx1*^{+/*mu*} chimaeric rat, whereas, in the *Pdx1*^{*mu*/*mu*} chimaeric rat, the PBS was retained in common bile duct and flowed backward to duodenum.



Extended Data Figure 6 | Analysis of transplanted islets. **a**, Bright-field (top) and fluorescent (bottom) images of hemi-nephrectomized kidney with (right) or without (left) transplanted islets. **b**, Transplanted islets, kidney capsule; anti-CD3 and -CD11b, hematoxylin counterstain. Islets lie inside the dotted line (Scale bars: 100 nm). **c**, Immunohistological analysis of engrafted islets under kidney capsule. Sections were stained with antibody against EGFP, insulin, glucagon and somatostatin and with DAPI. Scale bars, 100 nm. **d**, Quantitative analysis of sections of engrafted islets. Ratio of insulin-, glucagon- and somatostatin-positive cells were analysed by Image J software ($n = 3$). The mean values \pm s.d. were obtained

from 3 biological replicates ($P = 0.93$ insulin⁺ area in mouse^R islets versus in WT mouse islets; $P = 0.89$ glucagon⁺ area in mouse^R islets versus in WT mouse islets; $P = 0.77$ somatostatin⁺ area in mouse^R islets versus in WT mouse islets; Student's *t*-test). **e**, Top, FACS diagrams, dispersed small samples of WT rat kidney (left), WT mouse kidney (middle) and mouse kidney with transplanted islets (right). Cells were stained with fluorophore-tagged antibodies against mouse and rat CD31 (mCD31 and rCD31, respectively). Bottom, FACS diagram, EGFP expression by dispersed cells of mouse kidney with transplanted islets (right) ($n = 3$).



Extended Data Figure 7 | Analysis of mouse^R islets transplanted mice. **a**, AUC glucose, calculated from GTT data in Fig. 4d. The mean values ± s.d. were obtained from 3 independent experiments (*P* < 0.01 A, B or C versus D, E or F, Student's *t*-test). **b**, Nonfasting mouse c-peptide level (pmol l⁻¹) in serum from *Pdx1^{muA/muB}* + mPSCs chimaera, mouse transplanted with mouse^R islets, and C57BL/6 mouse. The lowest value of the *x* axis represent the lowest limit of detection. The mean values ± s.d. were obtained from 3 biological replicates except for *Pdx1^{mu/mu}* + mPSCs that was from 2 biological replicates (*P* < 0.01 *Pdx1^{mu/mu}* + mPSCs chimaera

and mouse^R islets transplanted mouse versus STZ treated mouse; *P* < 0.01 STZ treated mouse versus WT mouse; Student's *t*-test). **c**, Nonfasting rat c-peptide level (pmol l⁻¹) in serum of *Pdx1^{muA/muB}* + mPSCs chimaera, mouse transplanted with mouse^R islets, C57BL/6 mouse and Wistar rat. Values are mean ± s.d. N.D., not detected. The lowest value of the *x* axis represent the lowest limit of detection. The mean values ± s.d. were obtained from 3 biological replicates, except for *Pdx1^{mu/mu}* + mPSCs, for which they were obtained from 2 biological replicates.

Extended Data Table 1 | Sequence analysis of predicted off-target sites of *Pdx1* TALEN

		Wild type (Wistar rat) genome	
Symbol	chromosome#	locus	sequences
<i>Pdx1</i>	chr12	exonic	TGCGCACGGGTCCTTGTaagactgtgtggccgCGTAGTACTGCTCCTCA
<i>Clstn2</i>	chr8	intronic	TGCACACGAGTCCCTGAacattcctatagagagcaaaAGAAGTATTGCTCGTCC
<i>Adamts18</i>	chr19	intronic	TGCGCACACATACTTGTacgacacagaagctcagcTGAGGTATGGCTCCTCA
<i>Dpyd</i>	chr2	intronic	AGAAAAGCAGCACACCACcaggagccagataatcaggAGTAGAACTGTGCCTCA
<i>Zcchc7</i>	chr5	intronic	TGCACATGCATCCCTGTtaaggtctatcagagtgttttagAGTAGTAGTGTTTTCT
<i>Cpsf3</i>	chr6	intronic	TGAGCCCACTTCCTTGTgtgttaaaaagacactgaccgtgAGGAGTAATGCTCCTGG
<i>Nell2</i>	chr7	intronic	TAAGCAGAAGAATAAwTaccocagatccAGTAGTAGAGTTCCTCA
<i>Galnt13</i>	chr3	intronic	N. D.
<i>Dctn4</i>	chr18	intronic	TGGAGACCACTACTACTgttcttaattacagACATGGAGCCTAGCGTA
<i>Fhit</i>	chr15	intronic	TCAGGAGCAGGCCTACTcactatctgtgaagaagcATTGTTCTGGTCTGCA
<i>Mgp</i>	chr10	exonic	TGCGCCACGGAGTCTgttccatcagcaagtcgcccgaACAAGGACCTGTGGGA
<i>Lrba</i>	chr2	intronic	AACCCACAAGTCCCTTATggaataaaatctcactcAGAATTACTGCTAGTCA
<i>Fggy</i>	chr5	intronic	TGGRGAGCAGTAAAATGcagggtcagagctcttggggaAGAAGGGTGTGTGTGTG
<i>Slco6d1</i>	chr9	intronic	TGAATAGAAGTACTTCAtaaactgacaggataAGAATTATTGCTTCTCA
<i>Spred2</i>	chr14	intronic	CCCGCACAGATCCATCTctgtctggagaggtcaeccgcAGTAGTGTGGTCTCC
	chr12	intergenic	TGAGGAAAAGGCTGACTcagcaaaagtccctacctcacaaccACAAGGACCTGTGTCA
	chr12	intergenic	TGCCCAAAGTTCCTCGTtggttatgcccgtctctttgAGTTGTCTGCTACTCA
<i>Phka1</i>	chrX	exonic	TCCGGAGCATTTCGACTatcctctggtgtccagagccaAGTAGAACTGTGCTGG
<i>Olr1397</i>	chr10	exonic	TGCCCACTCTCCTTCTTgacactctgtttcaccAGTAGCACTGTCCCA
<i>Cks2</i>	chr17	exonic	TGCTCACCGTACTCGTagtctcgtcgaagtaactgtctgAGTAGTAGATCTGCTTG
	chr12	intergenic	TGAGAAACAGTACTCAagattgacctctggcctccatgctCATGTGCGCGTGCACA
<i>Wnt3a</i>	chr10	exonic	TTAGGAGCCCTCCTACTtgcagggtgcaagTCATAGACACGTGTGCA
<i>Pdx1+muA</i> genome			
Symbol			mutation type
<i>Pdx1</i>	sequences		2bp deletion
<i>Clstn2</i>	TGCACACGAGTCCCTGAacattcctatagagagcaaaAGAAGTATTGCTCGTCC		mutation (-)
<i>Adamts18</i>	TGCGCACACATACTTGTacgacacagaagctcagcTGAGGTATGGCTCCTCA		1bp substitution
<i>Dpyd</i>	AGAAAAGCAGCACACCACcaggagccagataatcaggAGTAGAACTGTGCCTCA		mutation (-)
<i>Zcchc7</i>	TGCACATGCATCCCTGTtaaggtctatcagagtgttttagAGTAGTAGTGTTTTCT		mutation (-)
<i>Cpsf3</i>	TGAGCCCACTTCCTTGTgtgttaaaaagacactgaccgtgAGGAGTAATGCTCCTGG		mutation (-)
<i>Nell2</i>	TAAGCAGAAGAATAAwTaccocagatccAGTAGTAGAGTTCCTCA		mutation (-)
<i>Galnt13</i>	N. D.		N. D.
<i>Dctn4</i>	TGGAGACCACTACTACTgttcttaattacagACATGGAGCCTAGCGTA		mutation (-)
<i>Fhit</i>	TCAGGAGCAGGCCTACTcactatctgtgaagaagcATTGTTCTGGTCTGCA		mutation (-)
<i>Mgp</i>	TGCGCCACGGAGTCTgttccatcagcaagtcgcccgaACAAGGACCTGTGGGA		mutation (-)
<i>Lrba</i>	AACCCACAAGTCCCTTATggaataaaatctcactcAGAATTACTGCTAGTCA		mutation (-)
<i>Fggy</i>	TGGGAGCAGTAAAATGcagggtcagagctcttggggaAGAAGGGTGTGTGTGTG		1bp substitution
<i>Slco6d1</i>	TGAATAGAAGTACTTCAtaaactgacaggataAGAATTATTGCTTCTCA		mutation (-)
<i>Spred2</i>	CCCGCACAGATCCATCTctgtctggagaggtcaeccgcAGTAGTGTGGTCTCC		mutation (-)
	TGAGGAAAAGGCTGACTcagcaaaagtccctacctcacaaccACAAGGACCTGTGTCA		1bp substitution
	TGCCCAAAGTTCCTCGTtggttatgcccgtctctttgAGTTGTCTGCTACTCA		mutation (-)
<i>Phka1</i>	TCCGGAGCATTTCGACTatcctctggtgtccagagccaAGTAGAACTGTGCTGG		mutation (-)
<i>Olr1397</i>	TGCCCACTCTCCTTCTTgacactctgtttcaccAGTAGCACTGTCCCA		1bp substitution
<i>Cks2</i>	TGCTCACCGTACTCGTagtctcgtcgaagtaactgtctgAGTAGTAGATCTGCTTG		mutation (-)
	TGAGAAACAGTACTCAagattgacctctggcctccatgctCATGTGCGCGTGCACA		mutation (-)
<i>Wnt3a</i>	TTAGGAGCCCTCCTACTtgcagggtgcaagTCATAGACACGTGTGCA		mutation (-)
<i>Pdx1+muB</i> genome			
Symbol			mutation type
<i>Pdx1</i>	sequences		8bp deletion
<i>Clstn2</i>	TGCACACGAGTCCCTGAacattcctatagagagcaaaAGAAGTATTGCTCGTCC		mutation (-)
<i>Adamts18</i>	TGCGCACACATACTTGTacgacacagaagctcagcTGAGGTATGCTCCTCA		1bp substitution
<i>Dpyd</i>	AGAAAAGCAGCACACCACcaggagccagataatcaggAGTAGAACTGTGCCTCA		mutation (-)
<i>Zcchc7</i>	TGCACATGCATCCCTGTtaaggtctatcagagtgttttagAGTAGTAGTGTTTTCT		mutation (-)
<i>Cpsf3</i>	TGAGCCCACTTCCTTGTgtgttaaaaagacactgaccgtgAGGAGTAATGCTCCTGG		mutation (-)
<i>Nell2</i>	TAAGCAGAAGAATAAwTaccocagatccAGTAGTAGAGTTCCTCA		mutation (-)
<i>Galnt13</i>	N. D.		N. D.
<i>Dctn4</i>	TGGAGACCACTACTACTgttcttaattacagACATGGAGCCTAGCGTA		mutation (-)
<i>Fhit</i>	TCAGGAGCAGGCCTACTcactatctgtgaagaagcATTGTTCTGGTCTGCA		mutation (-)
<i>Mgp</i>	TGCGCCACGGAGTCTgttccatcagcaagtcgcccgaACAAGGACCTGTGGGA		mutation (-)
<i>Lrba</i>	AACCCACAAGTCCCTTATggaataaaatctcactcAGAATTACTGCTAGTCA		mutation (-)
<i>Fggy</i>	TGGGAGCAGTAAAATGcagggtcagagctcttggggaAGAAGGGTGTGTGTGTG		1bp substitution
<i>Slco6d1</i>	TGAATAGAAGTACTTCAtaaactgacaggataAGAATTATTGCTTCTCA		mutation (-)
<i>Spred2</i>	CCCGCACAGATCCATCTctgtctggagaggtcaeccgcAGTAGTGTGGTCTCC		mutation (-)
	TGAGGAAAAGGCTGACTcagcaaaagtccctacctcacaaccACAAGGACCTGTGTCA		1bp substitution
	TGCCCAAAGTTCCTCGTtggttatgcccgtctctttgAGTTGTCTGCTACTCA		mutation (-)
<i>Phka1</i>	TCCGGAGCATTTCGACTatcctctggtgtccagagccaAGTAGAACTGTGCTGG		mutation (-)
<i>Olr1397</i>	TGCCCACTCTCCTTCTTgacactctgtttcaccAGTAGCACTGTCCCA		mutation (-)
<i>Cks2</i>	TGCTCACCGTACTCGTagtctcgtcgaagtaactgtctgAGTAGTAGATCTGCTTG		mutation (-)
	TGAGAAACAGTACTCAagattgacctctggcctccatgctCATGTGCGCGTGCACA		mutation (-)
<i>Wnt3a</i>	TTAGGAGCCCTCCTACTtgcagggtgcaagTCATAGACACGTGTGCA		mutation (-)

ND, not detected. Target sequence was impossible to amplify. Substitutions are indicated by red letters.